


Cite this: *RSC Adv.*, 2020, 10, 35848

# Development of an on-chip sample injection system with a 6-port valve incorporated in a microchip†

Kazuhiro Morioka,<sup>a</sup> Hina Sato,<sup>a</sup> Kenji Morita,<sup>a</sup> Hemmi Akihide,<sup>b</sup> Hizuru Nakajima,<sup>c</sup> Atsushi Shoji<sup>a</sup> and Akio Yanagida<sup>a</sup>

Micro-flow-injection analysis ( $\mu$ FIA) is amenable to high-throughput systems with lower consumption of sample and reagent volumes. On-chip sample injection methods are important to prevent reduced analytical performance associated with dead volumes and diffusion of sample solutions. In this study, we have developed an on-chip sample injection system with a small-sized 6-port valve incorporated on a microchip. The valve is made with a 3D printer and is a simple structure that can be easily operated manually. A sample solution in a loading channel can be injected by switching the valve from the load to injection position. Sample injection tests using resorufin solutions revealed that samples can be injected below  $100 \mu\text{L min}^{-1}$ , and the performance of the sample injection system is comparable to that of a commercially available injector. In addition, the sample injection system was successfully applied to a flow-based assay for hydrogen peroxide. The detection limit ( $3\sigma$ ) of hydrogen peroxide was estimated to be  $0.5 \mu\text{M}$ , and the assay time after sample injection was approximately 100 s. The developed sample injection system will be useful for various microfluidic-based analyses including  $\mu$ FIA.

Received 16th August 2020  
Accepted 18th September 2020

DOI: 10.1039/d0ra07043b

rsc.li/rsc-advances

## Introduction

Micro-flow-injection analysis ( $\mu$ FIA)<sup>1,2</sup> incorporates the flow injection analysis (FIA) method on a microfluidic device and is capable of high-throughput analysis because of the on-chip integration of analytical operations such as mixing,<sup>3,4</sup> reaction,<sup>5–7</sup> separation,<sup>8,9</sup> and detection.<sup>10–13</sup> On-chip integration is superior to conventional FIA methods as it reduces analysis time, as well as sample and reagent consumption. These advantages raise the possibility of analytical applications in diverse fields such as environmental testing,<sup>13–16</sup> medical diagnosis,<sup>8,16</sup> food analysis,<sup>17</sup> and drug testing.<sup>3,5,11</sup> However,  $\mu$ FIA systems are prone to suffering from reduced analytical performance resulting from dead volumes in the injection module and tubing connections more than conventional FIA systems.

To decrease the dead volume at the tubing connections between the microchip and the outside macro-world, some researchers have developed fluidic interconnection techniques,

such as a ball-joint connection,<sup>18</sup> an interference fit connection,<sup>19,20</sup> and connections using a convex-type or a long cast flange shaped polydimethylsiloxane (PDMS).<sup>21,22</sup> Further, van Swaay *et al.*<sup>23</sup> developed a simple and inexpensive chip-to-world connector with a sample injection port. Here, sample is added with a micropipette into a reservoir in the connector, and introduction of the sample to a microchannel was achieved by a syringe pump after sealing the reservoir with a sliding cap. The sample in the reservoir could be diluted with a carrier solution due to sample diffusion to the microchannel; however, this report indicated that an on-chip integration of a sample injection port was a very effective approach to introducing samples with low dead volumes.

Valve systems enable switching between load and injection modes without sample diffusion to a carrier solution because the loaded sample is isolated from the carrier solution until just before sample injection. Lab-on-a-disc<sup>24–27</sup> enables us to easily switch the flowing solution by controlling various valves and centrifugal force, but to flow the solution at the constant flow rate during rotation is difficult. Several research groups reported a platform of pinch-valve injections based on blockage of microchannels when loading a sample solution. External equipment is required to toggle the open/close state of the valves in these sample-introduction techniques, such as pressure-driven fluid flow utilizing gas<sup>28</sup> and liquid<sup>29–32</sup> feeding, channel switching with thermo actuated microvalves,<sup>33</sup> the control of electroosmotic flow direction in a straight-cross

<sup>a</sup>Department of Biomedical Analysis, School of Pharmacy, Tokyo University of Pharmacy and Life Sciences, 1432-1 Horinouchi, Hachioji, Tokyo 192-0392, Japan. E-mail: kmorioka@toyaku.ac.jp

<sup>b</sup>Mebius Advanced Technology Ltd., 3-31-6 Nishiogi-kita, Suginami-ku, Tokyo 167-0042, Japan

<sup>c</sup>Department of Applied Chemistry, Graduate School of Urban Environmental Science, Tokyo Metropolitan University, 1-1 Minami-ohsawa, Hachioji, Tokyo 192-0397, Japan

† Electronic supplementary information (ESI) available. See DOI: 10.1039/d0ra07043b



microfluidic chip by application of step-by-step voltage,<sup>34</sup> and flow switching with gravity-driven flow.<sup>35</sup>

Miniaturized valves have considerable promise as low-dead-volume injectors. External two-way valves connected to microchip reservoirs enable switching the sample load/injection modes, allowing injection of a sample in the nL to pL range due to the lower volume of the injection plug.<sup>36</sup> In this system, the operation of sample injection may be complex because of the combination of multiple two-way valves. Multi-port valves enable switching between sample loading and injection with a simple operation. In a 4-port valve developed by Su *et al.*,<sup>37</sup> a 5  $\mu\text{L}$  sample loaded in a sample loop within the valve was successfully introduced to the ICP-MS by turning the valve by 90°. Further, the sample injection module for cell analysis permitted the injection of 195 nL of sample loaded in a groove formed on a rotor structure.<sup>38</sup> These injectors with multi-port valves permit simple procedures for switching load/injection but also repetitive injection of different samples. However, sample load/injection systems with an external multi-port valve still have a dead-volume problem related to the parts connecting the valve and the microchip.

In this study, we propose an on-chip sample injection system with a 6-port valve incorporated in a microchip. The advantage of sample injection with the 6-port valve is capable of simple operation and the use of microchannel for sample loading. The microchip equipped with the valve was easily fabricated by inserting the valve in the hole of PDMS plate. The sample injection system can be easily operated by manually rotating the valve. The use of the valve stopper fixed on the microchip enables us to manually operate the valve with high repeatability. Sample injection with this system was demonstrated by observing the flow of visible dye solutions to a detection chamber. In addition, the system was applied to a flow-based assay for hydrogen peroxide.

## Experimental

### Principle of sample injection with a 6-port valve

The principle of on-chip sample injection is shown in Fig. 1. The 6-port valve with six liquid flow ports and three flow channels was inserted in a PDMS microchip. The flowing solution does not leak because of the elasticity of PDMS where the flow channel in the valve contacts the channel in the microchip.<sup>39</sup> When the valve is in the “Load” position, a carrier solution introduced from inlet 1 passes through one of the flow channels of the valve, and the solution is discharged from outlet 1. The loading channel is filled with a sample solution introduced through inlet 2 using a microsyringe. Switching from the “Load” to “Inject” mode is performed by rotating the valve by 60°. When the valve is in the “Inject” position, the carrier solution is introduced from inlet 1 with a microsyringe. The carrier solution passes through the loading channel and is finally discharged from outlet 1. At this time, the sample solution in the loading channel is ejected by the flow of the carrier solution, and the solution flows through a detection chamber.

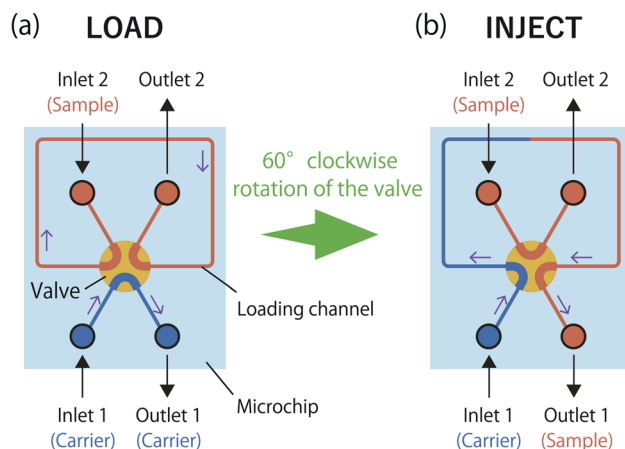


Fig. 1 Principle of the sample injection system using a 6-port valve. (a) Load mode. The carrier solution is introduced from inlet 1 and is discharged from outlet 1 after passing through a channel in the 6-port valve. The sample solution is introduced from inlet 2 into a loading channel. Excess sample solution is discharged from outlet 2. (b) Inject mode. When the valve is manually turned in the clockwise direction by 60°, the carrier solution flows into the loading channel, resulting in the sample solution being pushed along the loading channel. Therefore, the loaded sample solution flows toward outlet 1.

### Reagents and solutions

All chemical reagents used in this work were of analytical grade and water was purified by a Milli-Q® Reference (Nippon Millipore, Tokyo, Japan) system. ENG hard resin used for fabrication of the on-chip injector and a template for microfluidic device was obtained from Kudo 3D Inc. (CA, U.S.A.). Polydimethylsiloxane (PDMS) prepolymer and curing agent were purchased from Dow Corning Toray Co., Ltd. (Tokyo, Japan). Isopropyl alcohol (IPA), hydrochloric acid, sodium dihydrogen phosphate, disodium hydrogen phosphate, sodium chloride, ethanol and acetone were obtained from Kanto Chemical Co., Inc. (Tokyo, Japan). Tris(hydroxymethyl)aminomethane (Tris) was obtained from MP Biomedicals, Inc. (CA, U.S.A.). Food dyes (yellow and blue) were purchased from Kyoritsu Foods Co., Ltd. (Tokyo, Japan). Resorufin sodium salt and bovine serum albumin (BSA) were obtained from Sigma-Aldrich Co. LLC (MO, U.S.A.). Amplex Red was obtained from Thermo Fisher Scientific, Inc. (MA, USA). Hydrogen peroxide and horseradish peroxidase (HRP) were purchased from FUJIFILM Wako Pure Chemical Corp. (Tokyo, Japan).

### 6-Port valve design and fabrication

The 6-port valve was designed using the 3D CAD software “Fusion 360” (Autodesk, Inc., CA, U.S.A.). The design data were processed to create slice images using the free slicer software “Creation Workshop v1.0.0.75”. A structure including the 6-port valve and supports made of ENG hard resin was made by a DLP 3D printer “Titan 2-High Resolution” (Kudo 3D Inc., CA, U.S.A.) loaded the slice data. To remove unreacted resin, the structure was immersed in IPA for 3 min and then rinsed with sufficient amounts of fresh IPA. The structure was then dried at room temperature and the 6-port valve was completed by removing it



from the supports. Fig. 2a shows the design and a photograph of the 6-port valve. The 6-port valve is composed of a knob and a round pillar with liquid flow ports. The size of the pillar is 4.4 mm in diameter and 4 mm in length. A cross-sectional image of the flow channel in the valve was obtained using a scanning electron microscope (SEM) (S-3400N, Hitachi High-Technologies Corp., Tokyo, Japan) and is shown in Fig. 2b. The diameter of the liquid flow port and volume of the flow channel were estimated to be 700  $\mu\text{m}$  and 1.3  $\mu\text{L}$ , respectively. In addition, a valve stopper was fabricated using a similar process and enabled high repeatability of stopping the 6-port valve (Fig. 2c). The valve stopper has four round pegs (diameter of 1.65 mm, and length of 3.5 mm) for fixing on a microchip. Standard Triangulated Language (STL) files of the 6-port valve and the valve stopper can be found in ESI.†

### Microchip fabrication

Recently, microchip fabrication by a 3D printer have attracted attention.<sup>40</sup> Although PDMS microchips are commonly fabricated by a photolithography technique using SU-8, simple fabrication methods using 3D printers have been recently reported.<sup>41–43</sup> Here, we fabricated a microchip made of PDMS

using a template made with the DLP printing technique. An acrylic plate (60  $\times$  60  $\times$  3 mm) was attached to a hard resin container (Kudo 3D Inc., CA, U.S.A.) for the 3D printer with an acrylic/silicone double-sided adhesive sheet (3M Company, MN, U.S.A.), and a space between the acrylic plate and the container was filled with ENG Hard resin. The container was then placed on the 3D printer and a channel-shaped light beam was used to irradiate the resin for 12.5 s. The exposed resin cured, and the structure was formed on the acrylic plate. After peeling the structure from the container, the structure was washed with IPA and the adhesive sheet removed from the acrylic plate. The template was completed by drying the structure on the acrylic plate at room temperature and exposing to light emitted from a projector equipped in the 3D printer for 10 min. The PDMS prepolymer and the curing agent were mixed at a weight ratio of 10 : 1 and this mixture was poured into the template. After curing the mixture in a heating chamber (BR-43FL, Taitec Corp., Saitama, Japan) at 40  $^{\circ}\text{C}$  overnight, the PDMS plate replicating the structure of the channel was peeled from the template and was further cured in the heating chamber at 70  $^{\circ}\text{C}$  for 1 hour. Holes (1.5 mm diameter) for inserting PEEK tubes were then formed on the PDMS plate using a biopsy punch (BPP-15F, Kai Industries Co., Ltd., Tokyo, Japan). The textured PDMS plate and a flat PDMS plate were treated with a hand-held corona treater (BD-20AC, Electro-technic Products, IL, U.S.A.) and these were joined by heating in an oven (DK 600, Yamato Scientific Co., Ltd., Tokyo, Japan) at 120  $^{\circ}\text{C}$  for 1 hour. After the fused PDMS plate was cooled at room temperature, holes for inserting the pillar of the 6-port valve and the four pegs of the valve stopper were formed on the fused PDMS plate with biopsy punches (BP-L40K and BP-L15K, Kai Industries Co., Ltd., Tokyo, Japan). Finally, the microchip was completed by mounting the 6-port valve and the valve stopper, as shown in Fig. 3a. The design schematic and a photograph of the microchip are shown in Fig. 3b. The dimensions of the microchip are 41 mm in length, 23 mm in width, and 10 mm in height. The width and the depth of the channels are 263  $\mu\text{m}$  and 105  $\mu\text{m}$ , respectively. The volume of the loading channel is estimated to be 5.1  $\mu\text{L}$ . The microchip was washed with 1 M HCl solution, 1 M NaOH solution and ultrapure water before use.

### $\mu\text{FIA}$ system

The  $\mu\text{FIA}$  system (Fig. S1†) consisted of a syringe pump (SP-300, Next Advance Inc., NY, U.S.A.), the microchip, and a homemade fluorescence detection device. The device was composed of a 5 mm bullet-type ultra-high brightness green LED (OSPG5111A, OptoSupply Ltd., N.T., Hong Kong), a short-pass filter (SPF) (SVX570, Asahi Spectra Co., Ltd., Tokyo, Japan), a dichroic mirror (DM) (XF2029, Omega Optical, Inc., VT, U.S.A.), an objective lens (OL) (M Plan Apo 10 $\times$ , Mitsutoyo Corp., Kanagawa, Japan), a long-pass filter (LPF) (LVX590, Asahi Spectra Co., Ltd., Tokyo, Japan), and a photomultiplier (PMT) module (H10722-210, Hamamatsu Photonics K.K., Shizuoka, Japan). Fluorescence detected with the PMT module was converted to a voltage and transferred to a datalogger (ADC-24, Pico Technology, Cambridgeshire, U.K.). The datalogger was

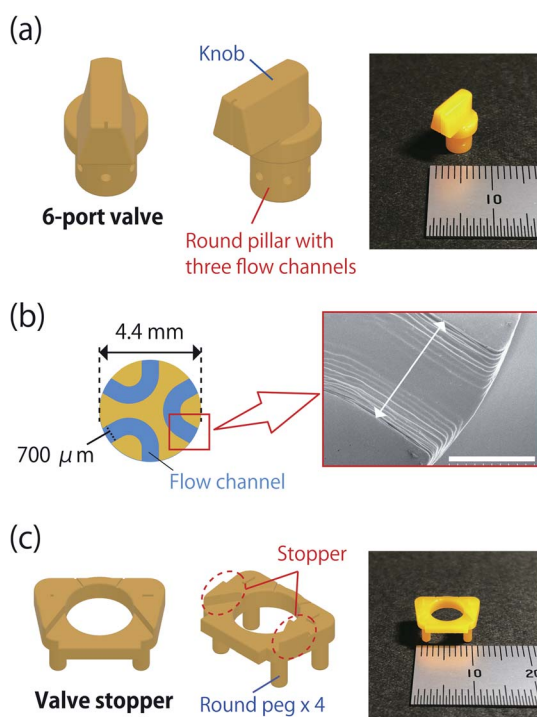


**Fig. 2** Six-port valve and valve stopper. (a) Drawings and a photograph of the 6-port valve. The microvalve has a knob for manual operation and a round pillar with three liquid flow channels. (b) A cross-sectional view depicting the arrangement of the six ports and three liquid flow channels. The pillar in the valve has three flow channels, each with a cross-sectional diameter of 700  $\mu\text{m}$ . The right panel is an SEM image of a cross-section of the pillar and flow channel. The white double-headed arrow indicates the diameter of the channel. The scale bar length is 500  $\mu\text{m}$ . (c) Drawings and a photograph of the valve stopper. The valve stopper has four pegs used to fix the stopper on a microfluidic device. The stopper functions to limit rotation of the valve to pre-determined positions.





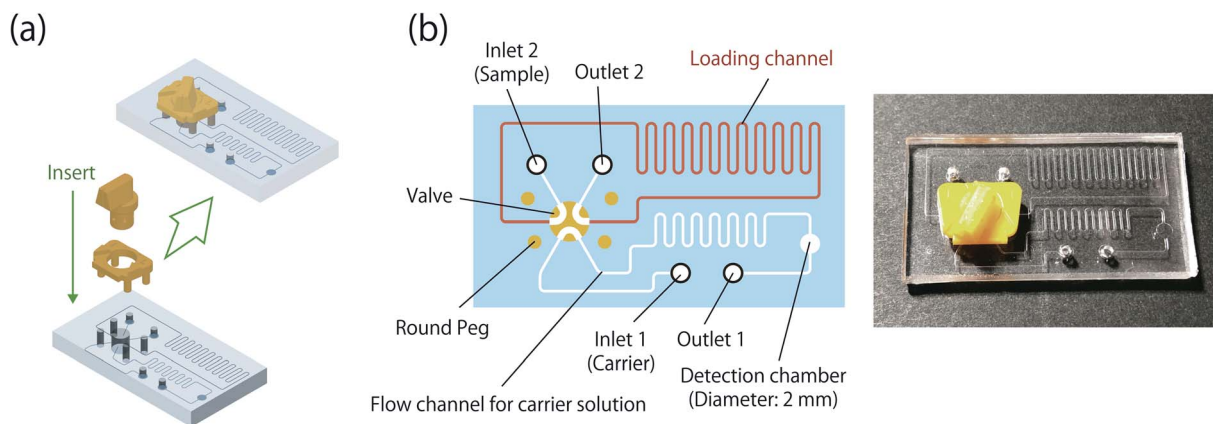


Fig. 3 The microchip equipped with the 6-port valve. (a) Schematic of integration of the valve and valve stopper on the microchip. (b) Cross-sectional drawing and photograph of the microchip equipped with the 6-port valve. The dimensions of the valve-equipped microchip are 41 mm in length, 23 mm in width, and 10 mm in height. The channels are 263  $\mu\text{m}$  in width and 105  $\mu\text{m}$  in depth.

connected to a notebook PC and the voltage was recorded by using PicoLog 6.1.9 software (Pico Technology, Cambridgeshire, U.K.). Fluorescence measurements were performed under the following conditions: the current of the LED was approximately 20 mA, and the sampling interval of the datalogger was set to 1 s. Details of the optical spectra used for the design of the device are shown in Fig. S2.†

### Hydrogen peroxide assay

A schematic illustration of the micro-flow-injection assay for the measurement of hydrogen peroxide is shown in Fig. S3.† Before the assay, the 6-port valve was immersed in 1% (w/v) BSA solution prepared in PBS (0.1 M sodium phosphate buffer containing 0.14 M NaCl; pH 7.4) for 30 min to prevent the nonspecific adsorption of proteins. A 10 ng mL<sup>-1</sup> HRP solution prepared in PBS was then introduced from outlet 1 with a microsyringe, and the region of a microchannel between the valve and outlet 1 was filled with the HRP solution. HRP was immobilized on an inner wall of the channel by incubation for 1 h at room temperature (RT). After the channel was washed with PBS, all channels were filled with the 1% BSA solution and then incubated for 30 min at RT. After incubation, the channels were thoroughly washed with a PB (50 mM sodium phosphate buffer; pH 7.4). The PB solution was used as a carrier solution and flowed at 10  $\mu\text{L min}^{-1}$  with a microsyringe pump, and a 10  $\mu\text{L}$  portion of a sample solution containing 100  $\mu\text{M}$  Amplex Red and hydrogen peroxide at known concentrations (0–1000  $\mu\text{M}$ ) was injected with a microsyringe.

## Results and discussion

### Demonstration of on-chip sample injection

A microchip with a hole formed at the intersection of two microchannels, *i.e.*, sample loading channel and flow channel for a carrier solution, was designed for the integration of a sample injection system on a microchip. A 6-port valve was inserted into the hole in the microchip, and the elasticity of PDMS enabled switching between the load and injection positions without the need for valve seals used in a conventional

valve injector. We optimized the diameter of the embedded round pillar of the 6-port valve to fit the 3.9 mm hole in the PDMS microchip (Fig. 2a). The valve performance was evaluated by water leakage from the microchip when the valve was switched from the load to injection position. With pillar diameters below 4.2 mm, the water leaked from the space between the pillar and the hole when rotating the valve. Moreover, distortion of the channel at the valve contact point was observed with a 4.6 mm diameter pillar. On the other hand, a valve with a 4.4 mm diameter pillar was able to switch between the load and injection positions without water leakage.

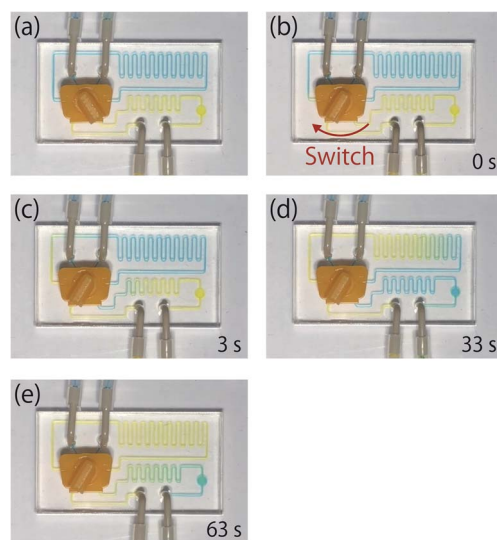


Fig. 4 Sequential imaging of dye solutions flowing through the channels. A carrier solution of 10% (w/v) yellow dye was flowed at 10  $\mu\text{L min}^{-1}$ , and a sample solution of 1% (w/v) blue dye was injected. (a) The carrier solution was flowed from inlet 1 and the sample solution was loaded from inlet 2 in load mode. (b) Load mode was switched to inject mode by turning the 6-port valve. (c) The carrier solution flowed into the loading channel, and the sample solution flowed into the channel with the detection chamber. (d and e) The sample solution reached the detection chamber and is ultimately discharged from outlet 2. The carrier solution gradually filled the loading channel over time.

In addition, the relationship of pillar and hole diameter was investigated, shown Fig. S4.† As a result, injection of water was achieved by all 6-port valves without water leakage. The experiments revealed that only 6-port valve with pillar diameter size in 0.5 mm larger than hole diameter permitted injection of water.

A flow test using dye solutions was carried out in order to verify the principle of the 6-port valve injector system. A 10% (w/v) aqueous yellow dye solution and a 1% (w/v) blue dye were used as carrier and sample solutions, respectively. Images of color changes in the microchip channels at various times following switching the valve are shown in Fig. 4. A video demonstrating the principle of sample injection is available in the ESI.† After switching the valve from load to injection, the loading channel was gradually filled with the yellow dye solution and the blue dye solution reached the detection chamber at approximately 26 s. After the detection chamber had been filled with the blue dye solution at approximately 50 s, the blue dye solution completely flowed out of the detection chamber. This result indicated that a sample solution could be injected into the channel with the developed system.

### Evaluation of the sample injection system

The durability of sample injection using the 6-port valve was evaluated by flow-injection and fluorescence measurement of resorufin. A Tris-HCl buffer solution containing 0.14 M NaCl; pH 8.0 (abbreviated as Tris buffer solution) was used as the carrier solution and was pumped at different flow rates, followed by injection of a 6.25  $\mu\text{M}$  resorufin solution. Fig. 5a shows the time profile of fluorescence responses observed at different flow rates. The sample was successfully injected below 100  $\mu\text{L min}^{-1}$ . Higher flow rates lead to sharp peaks, whereas trapezoidal peaks were observed at flow rates below 20  $\mu\text{L min}^{-1}$ . This result indicates that the 6-port valve can function appropriately over a range of flow rates often used in  $\mu\text{FIA}$ .<sup>44</sup> Flow rates above 20  $\mu\text{L min}^{-1}$  might reduce the reproducibility of analysis because injected samples reach the detection chamber virtually immediately and differences in the speed of manual valve turning could have a significant impact on the readout. In contrast, lower flow rates will decrease the throughput of the device. Therefore, a flow rate of 10  $\mu\text{L min}^{-1}$  was selected for further experiments.

Fig. 5b shows the fluorescence response obtained following repeated sample injection. The resorufin solution was injected 10 times at 300 s intervals. The relative standard deviation (RSD,  $n = 10$ ) calculated from the average fluorescence values observed during the 10 s time period of the plateau region of the trapezoidal fluorescence peak was estimated to be 1.3%. The result indicated that sample injection could be performed with high repeatability. However, an increase in the number of sample injections may cause a deterioration of the contacting surfaces of the 6-port valve and the valve stopper. To evaluate the deterioration in valve function due to repetitive sample injection, samples were injected following switching the valve between the load and injection positions 100 times. After repetitive valve turning, a sample was injected and

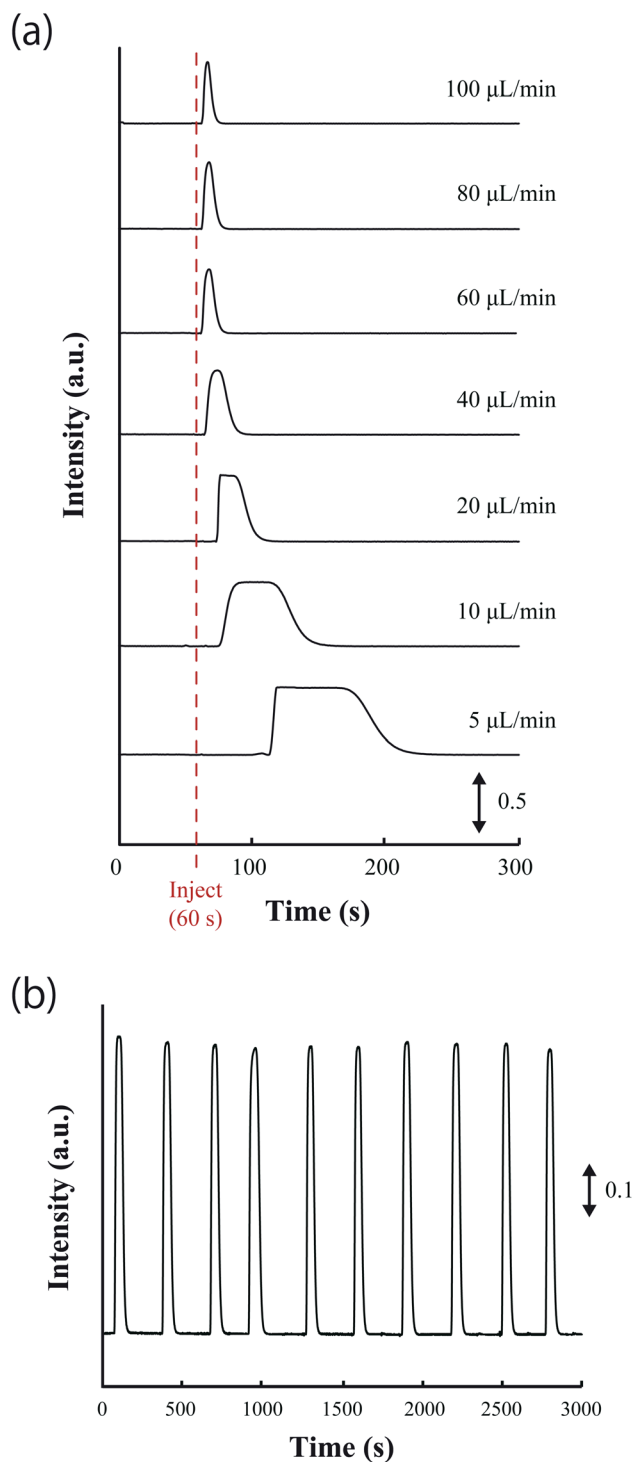


Fig. 5 Evaluation of sample injection using the 6-port valve. Tris buffer and 6.25  $\mu\text{M}$  resorufin were used as the carrier and sample solutions, respectively. (a) The figure shows the change in observed fluorescence over time at different flow rates. Sample solutions were injected 60 s after beginning fluorescent measurements. (b) The figure shows the fluorescent responses in the repeatability test. A sample solution was injected ten times at 300 s intervals.

a fluorescence response was obtained that was comparable to that without repetitive valve turning. This is because the contacting surfaces between the valve pillar and PDMS did not wear



down, which is attributable to the elasticity of PDMS. In addition, sample solution was successfully injected using the 6-port valve inserted in microchip stored over a year. This result

showed stress relaxation of PDMS did not affect to injection performance at least one year.

To investigate deterioration of injection performance caused by solution property, 1 M HCl aqueous solution (acidic solution), 1 M NaOH aqueous solution (alkaline solution), ethanol and acetone (organic solvents) were used as a sample solution. Firstly, the valve was immersed in each solution for one day. Significant changes of the valve in HCl, NaOH and ethanol solutions did not occur, but the valve immersed in acetone was decolorized and became brittle. Next, the solutions, except for acetone, were injected to a microchannel with the valve. HCl and NaOH solutions were successfully injected, but ethanol leaked between the valve and the PDMS. These experimental results show that the use of the valve is limited to aqueous solution.

### Comparison of sample injection using the 6-port valve and a commercial injector

Sample injection performance using the 6-port valve was compared to a commercial injector by measuring the fluorescence of resorufin. A Tris buffer solution was flowed as a carrier solution, and resorufin solutions were injected at 5 min intervals. Details of the commercial sample injection system are shown in Fig. S5.† Fig. 6a shows the fluorescence responses obtained using each injector system over time. Fluorescence peaks appeared at equal intervals, and fluorescence intensity increased according to the resorufin concentration. The shapes of the fluorescence signal peaks obtained using the 6-port valve were narrow trapezoids. With the commercial injector, a longer time period was required for the resorufin solution to reach the detection chamber since a 60 cm long PFA tube was used to connect the injector with the microchip. Moreover, the peak shape was broader and slightly lower due to sample diffusion occurring in the PFA tube and connectors.

This result revealed that the on-chip sample injection system is capable of effective sample introduction, with minimal diffusion and dead volume, suggesting that this system is useful for high-throughput analysis. Calibration curves for resorufin are shown in Fig. 6b, and a comparison of the performance of the sample injection methods is shown in Table 1. The calibration curves were linear over the measured concentration range. With measurements using the valve, the limit of detection (LOD) ( $3\sigma$ ) of resorufin and the RSD ( $n = 4$ ) in the detectable concentration range were estimated to be 78.6 nM and 10.5% or below, respectively. In comparison, measurements performed using the commercial injector yielded an LOD ( $3\sigma$ ) and RSD ( $n = 4$ ) of 138 nM and 9.1% or below, respectively. These results demonstrated that the performance of the valve sample injection system is comparable to that of the commercial injector.

### Hydrogen peroxide assay

The potential application of the sample injection system with the 6-port valve to  $\mu$ FIA was investigated by measuring hydrogen peroxide. A schematic illustration of the hydrogen peroxide measurement system is shown in Fig. S3.† The fluorescence intensity of resorufin generated by an enzymatic reaction was measured at the detection chamber during the flowing of

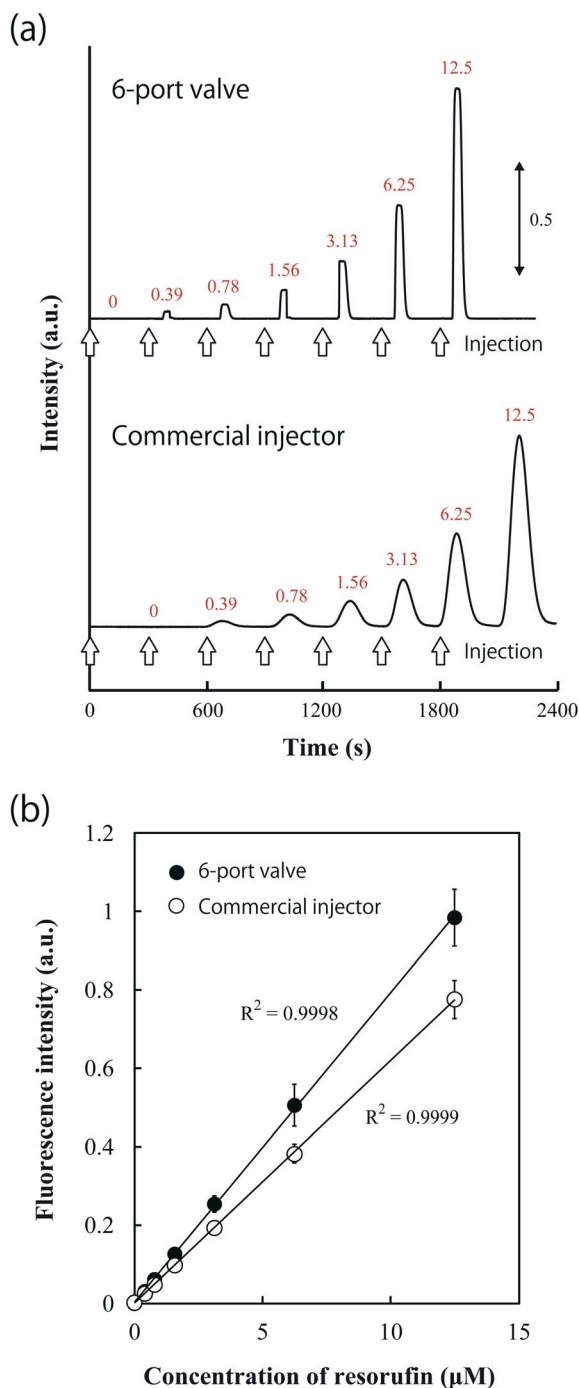


Fig. 6 Comparison of resorufin measurements following sample injection using the 6-port valve and a commercial injector. (a) Time-dependent changes in fluorescence measurements. Resorufin solutions of varying concentrations were injected at 300 s intervals. Red numbers indicate the concentration of the injected resorufin solution associated with each peak. (b) Calibration curves for resorufin. The fluorescence intensities represent the mean of a 10 s period of the plateau region of the response signal. Error bars indicate mean  $\pm$  standard deviation ( $n = 4$ ).



Table 1 Comparison of the performance of the 6-port valve and the commercial injector

	6-port valve	Commercial injector
LOD of resorufin ( $3\sigma$ ) (nM)	78.6	138
RSD ( $n = 4$ ) (%)	<10.5	<9.1
Dimension ( $L \times W \times H$ ) (mm)	$12 \times 9 \times 10$	$81 \times 35 \times 62$
Lightweight (g)	0.4	352 (without connectors and tubes)
Cost (\$)	0.054 (resin only)	652<

a carrier solution. The time-dependent changes in fluorescence are shown in Fig. 7a. Fluorescence intensity increased with increasing concentration of hydrogen peroxide, and Fig. 7b shows a calibration curve for hydrogen peroxide. The calibration curve at concentrations of less than  $31.3 \mu\text{M}$  showed good

linearity with a correlation coefficient of  $R^2 = 0.979$ . The LOD ( $3\sigma$ ) of hydrogen peroxide and the RSD ( $n = 4$ ) over the detectable concentration range were estimated to be  $0.5 \mu\text{M}$  and 12.1% or below, respectively. These results suggest that the microchip with the valve is well suited to flow injection-based assays. The time required from sample injection to detection of the full trapezoidal peak was approximately 100 s. This was attributable to the efficiency of the enzymatic reaction and on-chip sample injection. This result demonstrates that  $\mu\text{FIA}$  using the microchip embedded with the valve is suitable to being applied to rapid assay systems. Moreover, this sample injection method permits alteration of the injection volume by controlling the volume of the channel used for sample loading. Since the valve requires a small-footprint space for mounting on the microchip, the sample injection demonstrated in this study will be adapted to various microfluidic-based analyses in many fields.

## Conclusions

In this study, the sample injection system with a 6-port valve was developed. The sample injection system was demonstrated by observing the flowing of visible dye solutions. Sample injection with low dead volume was achieved without connecting parts by utilizing the elasticity of PDMS. The sample injection system was successfully applied to a flow-based assay for hydrogen peroxide. The valve is a simple structure, small-sized, durable, inexpensive, excellent in mass productivity, and disposable. Although valve switching for sample injection was a manual operation, this device is amenable to automation by combining the valve and a commercial servo actuator. Moreover, more than one valve can easily be integrated onto a single microchip. Since microchips with the valve can be designed according to specific applications and used easily, the sample injection method can be adapted to various microfluidic-based analyses in many fields such as environmental testing, medical diagnosis, food analysis, and drug discovery.

## Conflicts of interest

There are no conflicts to declare.

## Acknowledgements

This work was supported by Grant-in-Aid from the Japan Society for the Promotion of Science (JSPS) KAKENHI Grant Number (17K14504).

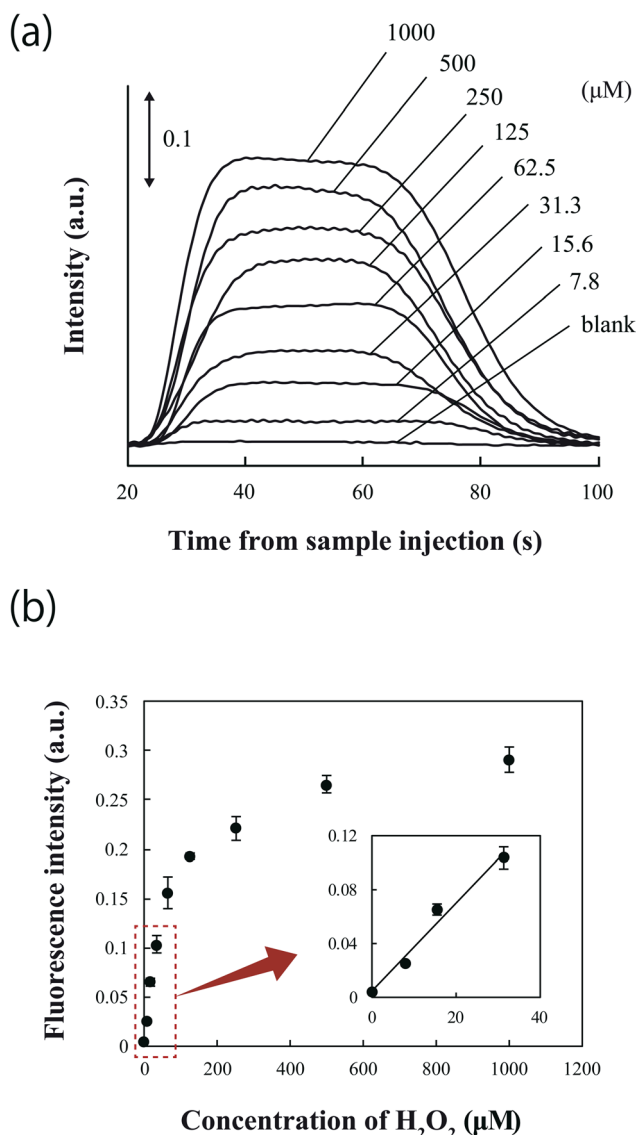


Fig. 7 Flow injection-based hydrogen peroxide assay. (a) Time-dependent changes in fluorescence intensities obtained by the measurement of varying concentrations of  $\text{H}_2\text{O}_2$ . (b) Plot of a  $\text{H}_2\text{O}_2$  calibration curve. The fluorescence intensities represent the mean of a 10 s period of the plateau region of the response signal. Error bars indicate mean  $\pm$  standard deviation ( $n = 4$ ).





## Notes and references

- 1 A. M. Leach, A. R. Wheeler and R. N. Zare, *Anal. Chem.*, 2003, **75**, 967–972.
- 2 W.-B. Du, Q. Fang and Z.-L. Fang, *Anal. Chem.*, 2006, **78**, 6404–6410.
- 3 H. Shen, B. Zhang, H. Xu, Y. Sun, Q. Wu, H. Shen and Y. Liu, *Pharm. Biomed. Anal.*, 2017, **134**, 333–339.
- 4 W. Khongpet, S. Pencharee, C. Puangpila, S. K. Hartwell, S. Lapanantnoppakhun and J. Jakmunee, *Talanta*, 2018, **177**, 77–85.
- 5 H. S. R. P. Moura, A. R. Mól, T. R. Sampaio and A. Fonseca, *Anal. Methods*, 2018, **10**, 5571–5576.
- 6 T. Ito, S. Kaneko and K. Suzuki, *Talanta*, 2011, **85**, 707–712.
- 7 Y.-T. Kim, S. O. Ko and J. H. Lee, *Talanta*, 2009, **78**, 998–1003.
- 8 S. Nishihama, H. Imabayashi, T. Matoba, C. Toya, K. Watanabe and K. Yoshizuka, *Talanta*, 2008, **74**, 1350–1354.
- 9 J. Wang and M. Pumera, *Talanta*, 2006, **69**, 984–987.
- 10 R. Liu, R. Ishimatsu, M. Yahiro, C. Adachi, K. Nakano and T. Imato, *Talanta*, 2015, **134**, 37–47.
- 11 X. Wang, M. Amatongchai, D. Nacapracha, O. Hofmann, J. C. de Mello, D. D. C. Bradley and A. J. de Mello, *Sens. Actuators, B*, 2009, **140**, 643–648.
- 12 F. M. Hernández-Maya and M. P. Cañizares-Macías, *Talanta*, 2018, **185**, 53–60.
- 13 P. H. Petsul, G. M. Greenway and S. J. Haswell, *Anal. Chim. Acta*, 2011, **428**, 155–161.
- 14 L. N. N. Nóbrega, L. O. Magalhães and A. Fonseca, *Microchem. J.*, 2013, **110**, 553–557.
- 15 B. Uthuppu, A. Heiskanen, D. Kofoed, J. Aamand, C. Jørgensen, M. Dufva and M. H. Jakobsen, *Analyst*, 2015, **140**, 1616–1623.
- 16 M. Miyake, H. Nakajima, A. Hemmi, M. Yahiro, C. Adachi, N. Soh, R. Ishimatsu, K. Nakano, K. Uchiyama and T. Imato, *Talanta*, 2012, **96**, 132–139.
- 17 D. He, Z. Zhang, Y. Huang and Y. Hu, *Food Chem.*, 2007, **101**, 667–672.
- 18 D. Sabourin, D. Snakenborg and M. Dufva, *Microfluid. Nanofluid.*, 2010, **9**, 87–93.
- 19 A. Pfreundt, K. B. Andersen, M. Dimaki and W. E. Svendsen, *J. Micromech. Microeng.*, 2015, **25**, 115010.
- 20 I.-H. Song and T. Park, *Micromachines*, 2019, **10**, 166.
- 21 V. Saarela, S. Franssila, S. Tuomikoski, S. Marttila, P. Östman, T. Sikanen, T. Kotiaho and R. Kostianen, *Sens. Actuators, B*, 2006, **114**, 552–557.
- 22 H.-I. Chang, F. Zhang, J.-I. Ding, S. Hong, M. Kraft and W. Yuan, *Microsyst. Technol.*, 2012, **18**, 723–730.
- 23 D. van Swaay, J.-P. Mächler, C. Stanley and A. deMello, *Lab Chip*, 2014, **14**, 178–181.
- 24 M. M. Aeinehvand, F. Ibrahim, S. W. Harun, A. Kazemzadeh, H. A. Rothan, R. Yusof and M. Madou, *Lab Chip*, 2015, **15**, 3358–3369.
- 25 A. Kazemzadeh, P. Ganesana, F. Ibrahim, M. M. Aeinehvand, L. Kulinsky and M. J. Madou, *Sens. Actuators, B*, 2014, **204**, 149–158.
- 26 W. Al-Faqheri, F. Ibrahim, T. H. G. Thio, M. M. Aeinehvand, H. Arof and M. Madou, *Sens. Actuators, A*, 2015, **222**, 245–254.
- 27 L. X. Kong, K. Parate, K. Abi-Samra and M. Madou, *Microfluid. Nanofluid.*, 2015, **18**, 1031–1037.
- 28 R. T. Kelly, C. Wang, S. J. Rausch, C. S. Lee and K. Tang, *Anal. Chem.*, 2014, **86**, 6723–6729.
- 29 A. L. Bowen and R. S. Martin, *Electrophoresis*, 2010, **31**, 2534–2540.
- 30 N. Y. Lee, M. Yanada and M. Seki, *Anal. Sci.*, 2004, **20**, 483–487.
- 31 S. Reichmuth, T. J. Shepodd and B. J. Kirby, *Anal. Chem.*, 2004, **76**, 5063–5068.
- 32 H. Moriguchi, T. Kawai and Y. Tanaka, *RSC Adv.*, 2015, **5**, 5237–5243.
- 33 Z. Li, Q. He, D. Ma and H. Chen, *Anal. Chim. Acta*, 2010, **665**, 107–112.
- 34 D. Sinton, L. Ren and D. Li, *J. Colloid Interface Sci.*, 2003, **266**, 448–456.
- 35 Y.-Z. Huang, W.-B. Du, J.-Z. Pan and Q. Fang, *Analyst*, 2008, **133**, 1237–1241.
- 36 A. P. O'Neill, P. O'Brien, J. Alderman, D. Hoffman, M. McEnery, J. Murrihy and J. D. Glennon, *J. Chromatogr. A*, 2001, **924**, 259–263.
- 37 C.-K. Su, S.-C. Hsia and Y.-C. Sun, *Anal. Chim. Acta*, 2014, **838**, 58–63.
- 38 S. Munshi, C. Chen, A. D. Townsend and R. S. Martin, *Anal. Methods*, 2018, **10**, 3364–3374.
- 39 M. T. Guler, P. Beyazkilic and C. Elbuen, *Sens. Actuators, A*, 2017, **265**, 224–230.
- 40 P. Liu, B. Li, L. Fu, Y. Huang, M. Man, J. Qi, X. Sun, Q. Kang, D. Shen and L. Chen, *ACS Sens.*, 2020, **5**, 464–473.
- 41 K. Kamei, Y. Mashimo, Y. Koyama, C. Fockenberger, M. Nakashima, M. Nakajima, J. Li and Y. Chen, *Biomed. Microdevices*, 2015, **17**, 36.
- 42 V. KaramZadeh, S. Foroughi, A. S. Kashani and M. Packirisamy, *Proceedings of the 5<sup>th</sup> International Conference of Fluid Flow, Heat and Transfer*, Niagara Falls, 2015, p. 172.
- 43 H. N. Chan, Y. Chen, Y. Shu, Y. Chen, Q. Tian and H. Wu, *Microfluid. Nanofluid.*, 2015, **19**, 9–18.
- 44 L. Ma, M. Oshima, S. Motomizu and T. Hattori, *Bunseki Kagaku*, 1998, **47**, 375–380.

